CLINICAL SCIENCES

INVESTIGATIVE NUCLEAR MEDICINE

Gated and Cinematic Perfusion Lung Imaging in Dogs with Experimental Pulmonary Embolism

Philip O. Alderson, Frank Vieras, Daniel F. Housholder, Karl G. Mendenhall, and Henry N. Wagner, Jr.

The Johns Hopkins Medical Institutions, Baltimore, Maryland, and the Armed Forces Radiobiology Research Institute, Bethesda, Maryland

To determine how pulmonary respiratory motion affects detection of pulmonary emboli, 11 dogs had routine lung scans and gated or cinematic perfusion images after undergoing autologous experimental pulmonary embolism. Six dogs had routine six-view perfusion studies, plus end-inspiratory and end-expiratory gated perfusion studies performed with a physiologic synchronizer set to 80% threshold. Five other dogs had three-view ungated and cinematic (post., LPO, RPO) perfusion images. Cinematic studies were acquired by synchronizing a camera-computer system to the Harvard respirator that ventilated the dog. Before death, all animals received i.v. India ink to outline pulmonary perfusion defects, and postmortem lung dissection verified sites of emboli. An ROC curve analysis of randomized perfusion studies showed that end-inspiratory gated images yielded true-positive rates 5–10% higher than ungated images at any given false-positive rate. Lesion detection by cinematic studies was comparable to detection by ungated images, but detection by end-expiratory images was worse. End-inspiratory gated imaging may be useful as an occasional adjunct to routine perfusion lung imaging.

J Nucl Med 20: 407–412, 1979

Radionuclide lung scanning is a sensitive procedure for the detection of perfusion defects caused by pulmonary emboli (*1–5*). However, a recent study of lung scanning in dogs with experimental embolism (*5*) revealed that emboli that occlude vessels smaller than 1 mm in size, or that block a vessel perfusing a zone smaller than 2 × 2 cm on the lung surface, are visualized infrequently. The lung scans performed in that study included both anterior and posterior oblique views, but no attempts were made to correct for the adverse effects of pulmonary motion on lesion detectability. Two techniques are available that might allow such corrections. Using gated acquisition, images could be obtained only during a specified, brief portion of the respiratory cycle such as end-inspiration or end-expiration. The image of that portion of the cycle alone would not contain significant respiratory motion. Alternatively, with the help of synchronized acquisition techniques, data could be acquired at frequent regular intervals throughout the respiratory cycle. Then, with the help of a small laboratory computer, these data could be displayed as a motion picture. Both these techniques have contributed to major advances in cardiac nuclear medicine (*6–8*), and

Received Oct. 27, 1978; revision accepted Dec. 19, 1978.

For reprints contact: Philip O. Alderson, Nuclear Medicine, Johns Hopkins Hospital, Baltimore, MD, 21205.

might also aid detection of pulmonary perfusion defects. This report describes results obtained with gated and cinematic perfusion lung imaging in dogs with pulmonary embolism.

METHODS

Pulmonary thromboemboli were experimentally produced in 11 dogs using a previously reported modification (5) of the technique of Wessler et al. (9,10). Each animal was anesthesized throughout the experimental procedure using i.v. pentabarbital (30 mg/kg). After intubation, the animal was placed supine on a small operating table, and cut-downs were performed on the right and left external jugular veins. Each vein was dissected free and a 3- to 4-cm segment was isolated with vascular clamps. Using a tuberculin syringe fitted with a 25-gauge needle, 50–100 NIH units of human thrombin were injected into each isolated vein segment. The isolated segment was then gently compressed to disperse the thrombin. After a 20-min waiting period, the vascular clamps were removed and the thrombi were released to the lungs. This procedure was performed twice in each animal.

Immediately after embolization, multiple-view perfusion images were obtained as described below. When the images were completed, the animal was placed supine and 10 cc of indelible commercial-grade India ink in 10 cc water were injected through the external jugular vein. Somlethol or potassium chloride was injected intravenously 1 min after the India ink. The total time from embolization to death was approximately 3 hr.

Each animal's chest was opened immediately after death and the trachea and pigmented lungs were removed. A tube was placed in the trachea and 10% buffered formalin was introduced into the bronchial tree by gravity feed until the lungs were inflated to their normal size. They were then placed in a large formalin-filled glass container and stored in a lead-shielded area. The next day the lungs were visually examined and any portion not pigmented (i.e., "perfusion defects") was noted, and its length and width measured. The lungs were then returned to the formalin-filled containers for at least 1 wk of additional fixation. The pulmonary vascular tree was then dissected and the sites and sizes of thrombi were noted. Only adherent clots were considered to be antemortem.

Data acquisition and display. Gated perfusion lung images were obtained in six dogs. Immediately after embolization, each dog received a 2- to 3-mCi i.v. injection of Tc-99m macroaggregated albumin (MAA). Perfusion images were obtained using a gamma camera fitted with a high-resolution parallel-hole collimator. The electrodes from a physiologic synchronizer* were attached to each side of the dog's thorax, and the gate was set to an 80% threshold. The first image was then obtained from the posterior projection with the synchronizer operating in the inspiratory mode. Thus, the camera acquired data only during 20% of the respiratory cycle centered about peak inspiration. When the end-inspiratory posterior image was completed, the gating process was repeated with the synchronizer in the expiratory mode. Finally, without changing the dog's position, the image was acquired in standard ungated fashion. This process was repeated for each of six perfusion views (including left and right posterior obliques). During these studies, the dogs were breathing spontaneously at a rate of 15–20 breaths per minute, and no artificial means were used to increase the size of a tidal breath (usually 200–400 cc). Each end-inspiratory image required a 10–12 min acquisition time. All gated and ungated images were recorded on Polaroid film at the same camera intensity setting. All images contained 400K counts. No digital data were acquired during these studies.

In five other dogs, peak inspiration was used as a gating signal and digital data were acquired throughout the respiratory cycle. After embolization and injection of 4–5 mCi of Tc-99m-labeled microspheres, each intubated anesthesized dog was attached to a Harvard respirator that delivered 500-cc inspirations at a regular rate of 15 per minute. Each time the piston of the Harvard respirator reached its maximum excursion (i.e., peak inspiration) it made contact with an electrode wired into a digital computer.† This contact served as the signal for the computer to begin a respiratory cycle. The computer divided each cycle into 14 intervals. Four million total counts per view were acquired from approximately 200 respiratory cycles (roughly a 15-min acquisition time). Three views (post., RPO, LPO) were obtained during these studies, which were done using a large-field-of-view gamma camera fitted with a high-resolution parallel-hole collimator. Routine, unsynchronized 400,000-count images were acquired simultaneously on 35-mm film. The digital data were displayed as a continuously cycled motion picture during the image-analysis phase of the study.

Data analysis. The end-inspiratory, end-expiratory, and routine (ungated) images were evaluated by two independent observers who did not know the results from the India-ink preparation or postmortem dissection. Each observer interpreted three six-view lung scans for each of the six animals. These 18 lung scans were presented in randomized order to the observers. Neither the dog number nor type of data acquisition (i.e., gated or ungated) was

revealed. The observers analyzed each bronchopulmonary segment and decided whether a perfusion defect was present. Throughout the study, the lobar anatomy was described using terminology applied to human lungs. Thus, the upper lobes corresponded to the canine apical lobes; the lower lobes to the diaphragmatic lobes; the right middle lobe to the right intermediate and cardiac lobes; and the lingula to the left cardiac lobe. The left lung thus contained nine bronchopulmonary segments and the right lung ten. The observers rated the degree of confidence associated with each reading on a 0–4 scale: 0 = definitely no defect, 1 = probably no defect, 2 = uncertain, 3 = probably a defect, 4 = defect definitely present. Their readings were then compared with the results of the India-ink preparation and postmortem dissection. The true- and false-positive rates for each observer's readings were determined and the results combined in a receiver-operating characteristic (ROC) analysis for each type of image acquisition.

A similar independent analysis was performed to compare routine and cinematic display in the other five dogs (total scans = ten). In this comparison, the type of data acquisition was obvious to the observers, but the studies were still read in randomized order and the dog numbers were not identified. The cinematic studies were viewed directly on the computer's output oscilloscope as uninterpolated 64 × 64 digital images. Variable degrees of contrast enhancement and cinematic display speed (to the observer's preference) were used to aid lesion detection. These readings were then used to construct ROC curves as described above.

In a separate analysis, the observers' subjective opinions concerning the clarity of perfusion defects were investigated. This study involved side-by-side comparisons of ungated, end-inspiratory and end-expiratory Polaroid images, plus a set of control images obtained after death of the dogs. Each observer was presented with 36 sets of these four types of images arranged on cardboard film holders. Each set contained four images of the same projection (e.g., four anterior views, four posterior views, etc.). The type of image acquisition was not identified, and care was taken to randomize the positions of the various types of images on the cardboard holders—i.e., images acquired in each manner appeared randomly in any of the four positions on the cardboard film holder. Each observer then independently rated the images for defect clarity. Most of the images contained multiple perfusion defects, but the observer's rating in this portion of the study was based on his impression of overall image clarity. The best image in a set was scored 4, the next best 3, then 2, and the worst was given a score of 1. If images were of equal quality, the same score could be given. Only integer scores could be used. The maximum score per observer for each imaging modality was 144 points. This is based on a score of 4 in each of six views per animal, times six animals (24 × 6 = 144). Since two observers were involved in this analysis, the total perfect score was 288. This study was done after the ROC analysis to avoid any bias that might be introduced by side-by-side image comparisons. The results of the ROC analysis were not revealed to the observers until after the image-clarity comparisons had been completed.

RESULTS

Pulmonary thromboemboli were present in each of the 11 dogs, as documented by the India-ink preparation and postmortem lung dissection. There were 51 emboli in the six dogs that had gated perfusion lung images (six to 11 emboli per dog), and 36 emboli in the five dogs that had cinematic lung images (five to eight emboli per dog). Thus, for each gated analysis compared with routine ROC analysis, the observers made decisions about 228 segments (19 per dog × 6 dogs × 2 observers), and 43% were abnormal. For the cinematic analysis compared with routine analysis, they made decisions on 190 segments, 40% containing emboli. The right and left lungs were embolized with roughly equal frequency (46% left and 54% right). The lower lobes contained nearly two-thirds of all emboli, with the lateral and posterior segments being the most frequent sites.

Cinematic display of perfusion lung images revealed two types of motion occurring at the edges of perfusion defects created by the autologous pulmonary emboli. The primary motion was in the apical-to-base axis. The defects moved downward as the lung expanded during inhalation and moved upward during exhalation. In addition, perfusion defects expanded during inhalation as air entered the involved pulmonary segments. Thus, the opposing edges of perfusion defects were moving apart and downward during inhalation. This motion was most easily visualized in defects that occurred in the lower lobes.

Figure 1 shows the ROC curve analysis of simultaneously acquired three-view cinematic and routine lung images. For any given false-positive rate (FPR), the cinematic curve had a higher true-positive rate (TPR), but the differences were minimal. The curve for the routine lung images showed relatively poor sensitivity. This was probably because these were three-view rather than six-view perfusion lung studies.

Figure 2 shows the ROC curve analysis compar-

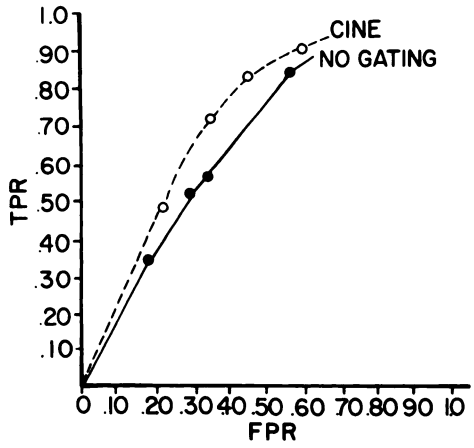

FIG. 1. ROC curve analysis of cinematic perfusion lung images (interrupted curve, open circles) vs. ungated images (solid line, closed circles) is shown. TPR and FPR are true- and false-positive rates, as determined from India-ink preparations and postmortem dissection.

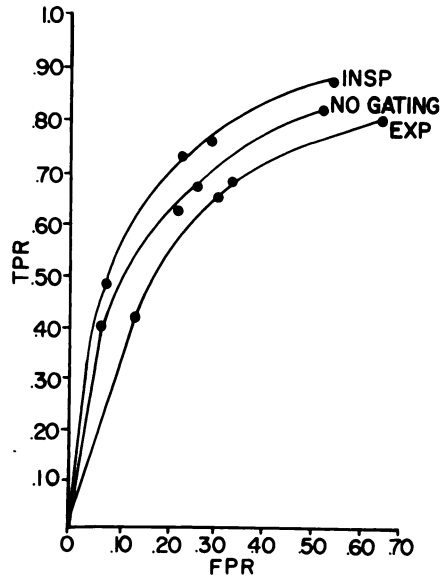

FIG. 2. ROC curve analysis of end-inspiratory gated images (INSP) vs. end-expiratory gated images (EXP) and standard ungated images is shown. TPR and FPR are true- and false-positive rates, as determined from India-ink preparations and post-mortem dissection.

ing routine six-view lung images with images obtained only during end-inspiration or end-expiration. The uppermost curve was obtained from the images gated in end-inspiration. The sensitivity (TPR) of end-inspiratory images exceeded that of routine images by 5–10% for any given specificity (FPR). The poorest results were obtained from end-expiratory gated images, which demonstrated lower sensitivity (TPR) than routine images at all levels of specificity (FPR).

As expected from the findings of cinematic display, perfusion defects seemed larger on end-inspiratory images (Fig. 3). In certain views, this led to a defect's being seen only on the end-inspiratory image, but other gated and routine views in the same animal usually revealed the defect. Five embolic perfusion defects were seen only on the end-inspiratory studies. The sizes of these five defects, as determined from the India-ink preparations, and their lobar locations, are shown in Table 1. Two of the defects were only suggested (i.e., an "unlikely" rating) on the end-inspiratory images, but three were diagnosed with confidence. In retrospect, however, each of these defects was visible in the ungated images. In addition, each of these defects was seen in the ungated images by one of the two observers. No defect that was missed by both observers on the ungated studies was seen on the end-inspiratory images.

Five of nine perfusion defects that measured less than 2 × 2 cm on the lung surface, as determined from the India-ink preparation, were seen with greater confidence in the end-inspiratory images. Four of these five were visualized with low confidence (0–2 rating) on the ungated study and high confidence (3–4 rating) on the end-inspiratory study. However, gating also led to increased detec-

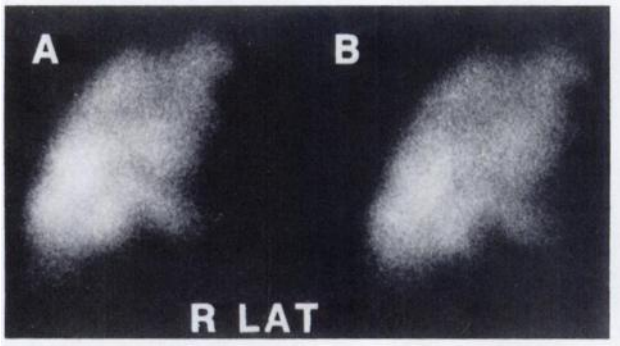

FIG. 3. Ungated (A) and end-inspiratory (B) right lateral images of a dog with a 2- by 4.2-cm India-ink defect in anterior segment of right lower lobe, a 2.7- by 3-cm defect in right middle lobe, and a 2.5- by 5-cm defect in apical segment of right upper lobe are shown. Note increased sizes of defects in end-inspiratory image.

TABLE 1. DEFECTS VISUALIZED ONLY ON END-INSPIRATION IMAGES

Location	Size	Confidence
Ant seg RUL	2.6 × 3.5	1
Ant seg RUL	2.4 × 1.5	1
Rt middle lobe	3.2 × 4.8	4
Ant seg RLL	2.1 × 3.6	4
Post seg LLL	1.6 × 0.5	4

tion confidence in some larger lesions. The mean area of defects (n = 22) seen with equal confidence on ungated and end-inspiratory images was 14.1 cm^2 ± 13.1 cm^2 s.d. Defects seen with greater confidence on end-inspiratory images (n = 29) had a mean area of 10.4 cm^2 ± 5.4 cm^2 s.d. ($t = 1.38$, $p > 0.2$). The smallest mean area (8.8 cm^2 ± 5.3 cm^2 s.d.) was found in the subset of 14 defects given a low probability rating (0–2) on ungated images, but a high probability rating (3–4) on the end-inspiratory study. However, this group of defects was not significantly smaller ($t = 1.43$, $p > 0.2$) than the group detected with equal confidence on gated and ungated studies.

The subjective scores of image clarity for the studies acquired on Polaroid film showed that the observers preferred gated perfusion images. The cumulative score for gated end-inspiratory plus gated end-expiratory images in the 72 image sets was 264, compared with a score of 149 for ungated images (a perfect score for a single imaging modality was 288). The gated images were scored higher than ungated studies in each of the six dogs. The observers were evenly divided concerning which type of gated image provided the best clarity. The total scores for end-inspiratory and end-expiratory images were 184 and 180, respectively.

DISCUSSION

Perfusion lung scanning is a sensitive test for pulmonary embolism. In 1970, Poulouse et al. (*1*) reported the angiographic and lung-scan findings in 108 patients with suspected embolism. Twenty-one patients had normal perfusion lung scans, and none had specific angiographic evidence of emboli. Since that time, no verified reports have appeared of angiographic detection of emboli in patients with normal lung scans. However, Moser et al. (*2*) demonstrated that perfusion lung scans in dogs with experimentally induced emboli failed to detect some embolic sites that could be visualized angiographically. We recently extended this work by comparing the results of selective pulmonary angiography with eight-view gamma-camera perfusion lung scans performed in dogs that had received autologous emboli (*5*). Only three of nine emboli that occluded pulmonary vessels less than 1 mm in diameter were visualized by the scans. When vessels 1.1 to 2.0 mm in diameter were occluded, 18 of 23 emboli (78%) were seen in the lung scan. When the occluded vessel was larger than 2 mm, 36 of 37 emboli (97%) were visualized. These experimental data suggest that the lung scan may be relatively insensitive to the smallest, most peripheral emboli. Since the lung is moving through the respiratory cycle during imaging, it seemed possible that motion could degrade image sharpness and account, in part, for the results of these experimental studies.

Gated or physiologically synchronized radionuclide images have been used in attempts to improve lesion detection in other organs. Myocardial Tl-201 images and liver scans are obtained using tracers that accumulate in the normal tissue of the organ. Lesions are revealed as defects in activity. Turner et al. (*11*) did an ROC analysis of randomly selected liver scans, performed with Tc-99m sulfur colloid and an electronic motion-correction device, and found significant improvements over routine liver imaging. However, Neumann et al. (*12*) performed a similar study and their analysis of equivocal liver scans demonstrated no increases in accuracy from motion correction. Goble et al. (*13*) compared end-diastolic-gated Tl-201 images with routine images and cinematic display in a mechanical heart model containing resin disk "cardiac lesions." An ROC analysis revealed significantly improved lesion detection with the cinematic and gated displays. Hamilton et al. (*14*) found that myocardial Tl-201 perfusion defects in patient studies were more readily apparent in motion-free ECG-synchronized images than in standard unsynchronized images, but other investigators (*15*) found no difference between lesion detection rates in patients studied by both cinematic and standard Tl-201 imaging techniques. McKusick et al. (*16*) found that end-diastolic images provided increased certainty of detection in patient studies, but revealed no lesions not visualized on ungated Tl-201 images. Thus, the results of gating and cinematic studies in detecting hepatic and myocardial defects have been inconsistent.

The results of the current study suggest that detection of pulmonary perfusion defects can be enhanced by gating, but the gains in detectability are modest. The study does demonstrate that the end-inspiratory phase, when the size of perfusion defects is maximal, provides good image clarity and the highest detection sensitivity. The importance of the size of the image defect is emphasized by the relatively poor results obtained in end-expiratory images. Even though these images had good clarity, the ROC analysis revealed substantially better observer performance using end-inspiratory images. This also emphasizes the importance of ROC analysis in this type of research. Even though subjective estimates of clarity revealed no difference between end-inspiratory and end-expiratory images, the ROC analysis showed that end-inspiratory gating was clearly superior to end-expiratory imaging for defect detection.

The results obtained with cinematic imaging were

disappointing. The ROC curves for cinematic and ungated images were similar. This is partly because the cinematic images were viewed in a noninterpolated 64 × 64 matrix format. The block-like image quality detracted from the edge-enhancing capabilities of a cinematic display. Further research with interpolated images in a larger matrix should be done to evaluate this technique more fully.

The cinematic images did reveal that perfusion defects distal to emboli "open" during inspiration, in addition to their downward movement. This suggests a possible application of these images to the specificity problem in diagnosing emboli. Would perfusion defects caused by airways disease show this obvious "opening" at peak inspiration? Zones with poor ventilation would not be likely to have this appearance. Thus, it is possible that perfusion defects caused by emboli could be distinguished from those occurring secondary to airways disease by the presence or absence of normal defect expansion during inspiration. This possibility merits further study.

The results of the current study suggest that gated end-inspiratory lung imaging may have clinical utility. However, the combination of increased imaging time and modest gains in defect detectability suggest that the current role is an adjunctive one. The technique could be used to clarify ill-defined defects in certain views of selected patients. The gating instrumentation required is widely available, and no other special equipment or computers are needed. In patients who can hold their breath, an image accumulated during several intervals of breath holding at deep inspiration might serve as a simple, but less well-controlled, alternative to a gated end-inspiration image.

FOOTNOTES

* Brattle Instrument Company

† Ohio Nuclear VIP

* Research was conducted according to the principles enunciated in the "Guide for the Care and Use of Laboratory Animals," prepared by the Institute of Laboratory Animal Resources, National Research Council.

ACKNOWLEDGMENTS

We thank Edward Barron, Michael Flynn, and John Warrenfeltz at AFRRI, and Thomas Wainwright at the Johns Hopkins Medical Institutions, for their technical assistance in performing the animal studies.

This work was supported in part by USPHS Grant GM-10548.

REFERENCES

1. POULOUSE KP, REBA RC, GILDAY DL, et al: Diagnosis of pulmonary embolism. A correlative study of the clinical, scan and angiographic findings. *Br Med J* 3: 67–71, 1970
2. MOSER KM, HARSAYANI P, RIUS-GARRIGA G, et al: Assessment of pulmonary photoscanning and angiography in experimental pulmonary embolism. *Circulation* 39: 663–674, 1969
3. MCNEIL BJ, HOLMAN BL, ADELSTEIN SJ: The scintigraphic definition of pulmonary embolism. *JAMA* 227: 753–756, 1974
4. MOSES DC, SILVER TM, BOOKSTEIN JJ: The complementary roles of chest radiography, lung scanning, and selective pulmonary angiography in the diagnosis of pulmonary embolism. *Circulation* 49: 179–188, 1974
5. ALDERSON, PO, DOPPMAN JL, DIAMOND SS, et al: Ventilation-perfusion lung imaging and selective pulmonary angiography in dogs with experimental pulmonary embolism. *J Nucl Med* 19: 164–171, 1978
6. ZARET BL, STRAUSS HW, HURLEY PJ, et al: A noninvasive scintiphotographic method for detecting regional ventricular dysfunction in man. *N Engl J Med* 284: 1165–1170, 1971
7. PITT B, STRAUSS HW: Evaluation of ventricular function by radioisotopic technics. *N Engl J Med* 296: 1097–1099, 1977
8. BORER JS, BACHARACH SL, GREEN MV, et al: Real-time radionuclide cineangiography in the noninvasive evaluation of global and regional left ventricular function at rest and during exercise in patients with coronary-artery disease. *N Engl J Med* 296: 839–844, 1977
9. WESSLER S, WARD K, HO C: Studies in intravascular coagulation. III. The pathogenesis of serum-induced venous thrombosis. *J Clin Invest* 34: 647–651, 1955
10. WESSLER S, FREIMAN DG, BALLON JD, et al: Experimental pulmonary embolism with serum-induced thrombi. *Amer J Path* 38: 89–101, 1961
11. TURNER DA, FORDHAM EW, ALI A, et al: Motion corrected hepatic scintigraphy: An objective clinical evaluation. *J Nucl Med* 19: 142–148, 1978
12. NEUMANN RD, GOTTSCHALK A, HOFFER PB: Electronic motion-correction in equivocal liver scans. *J Nucl Med* 19: 737, 1978
13. GOBLE JC, WAGNER HN JR, ALDERSON PO, et al: Factors affecting perception of myocardial perfusion defects using Tl-201. *J Nucl Med* 19: 679–680, 1978 (abst)
14. HAMILTON GW, NARAHARA KA, TROBAUGH GB, et al: Thallium-201 myocardial imaging: characterization of ECG-synchronized images. *J Nucl Med* 19: 1103–1110, 1978
15. ALDERSON PO, WAGNER HN JR, GOMEZ-MOEIRAS JJ, et al: Simultaneous detection of myocardial perfusion and wall motion abnormalities by cinematic ^{201}Tl imaging. *Radiology* 127: 531–533, 1978
16. MCKUSICK KA, BINGHAM J, POHOST G, et al: Comparison of defect detection on ungated vs. gated thallium-201 cardiac images. World Fed Nuc Med Biol. Second International Congress, September 17–21, 1978, Washington D.C., p 50 (abst)